3

Mechanisms of Relative Sea-level Change and the Geophysical Responses to Ice-water Loading

W.R. Peltier

INTRODUCTION

The classification of mechanisms of sea-level change

The purpose of this chapter is firstly to provide a discussion of the variety of mechanisms which may cause changes in sea level, particularly those associated with the melting of continental ice sheets. Secondly, detailed consideration will also be given to some examples of what has been learnt about the earth and the operation of its climate system through the analysis of observations of such changes.

The physical mechanisms which are responsible for causing variations of sea level are clearly a strong function of the timescale on which the change occurs. Because most measurements of sea-level change, regardless of the timescale of the variability, are taken relative to the surface of the solid earth, it is useful in discussing mechanisms to distinguish the changes to which they give rise as belonging to one or the other of two classes. These classes are conventionally labelled *eustatic* and *isostatic*. The appearance of the root 'static' in both these words is meant to imply that the changes referred to are quasi-permanent and to be distinguished from the more ephemeral and quasi-periodic variations associated with oceanic tides and with the annual fluctuation of sea level which follows the seasonal climate cycle.

In the discussion which follows the word *eustatic* will be used to describe changes in sea level which are a consequence of a change in the volume of the water in the global ocean or in some local part of it. Such eustatic changes may be a consequence either of a change in ocean mass (caused, say, by the accretion or melting of continental ice sheets), or of a change in the volume which a fixed mass occupies through so-called *steric* effects associated for example with variations of temperature and the process of thermal expansion (caused, say, by a change of global climate). In the literatures of hydrodynamics and oceanography the words *barotropic* and

baroclinic are also employed to denote respectively the non-steric and steric components of the eustatic sea-level change and these words will be used interchangeably in the following discussion.

The *isostatic* contribution to the local variation of sea level is completely distinct from this eustatic component with its barotropic and baroclinic constituents. Just as eustatic changes are associated with changes of ocean volume, so isostatic changes are caused by predominantly radial displacements of the surface of the solid earth. Since sea-level change is normally observed relative to this surface it is clear that every such observation is inherently ambiguous. If one observes an increasing relative sea level in some particular geographic location this could be due, in principle, either to an increase in the local height of the water column (a eustatic effect) or to a decrease in the local radius of the solid earth (an isostatic effect). Much of the challenge in the analysis of relative sea-level data lies in attempting to separate these two fundamentally different contributions to observations of relative sea-level change. From the eustatic component comes information on the nature of climate change, whilst from the isostatic contribution comes information concerning the nature of the solid earth. In what follows an attempt will be made to provide some examples of both types of information to illustrate the nature of sea-level data itself, as well as the specific questions which it may be employed to address.

THE MECHANISMS AND THEIR ASSOCIATED CHANGES OF SEA LEVEL

Short timescale mechanisms

Probably the most dramatic mechanism contributing to relative sea-level variations in a few special locations is that associated with earthquakes. Of course such events occur on an extremely short timescale, usually a small fraction of a minute, and significant effects on the sea-level record are found only when the earthquake is located offshore and has an appreciable 'dip-slip' component of its source mechanism. When these two conditions are satisfied, and the rupture actually extends to the earth's surface, then associated with the earthquake there is a relative vertical motion of the sea floor on either side of the fault break. This may extend onshore, where it will be registered as a change of relative sea level on a tide gauge attached to the surface of the solid earth. Besides this semi-permanent isostatic change in sea level, associated with the induced vertical displacement of the surface of the solid earth, such earthquakes also give rise to intense transient variations of relative sea level. These travel away from the epicentre as water waves called *tsunamis* which can cause extreme damage when they propagate onshore at distant locations. Although the amplitude

of the relative sea-level (RSL) change associated with the tsunami is only of the order of 1 cm in the open ocean, it may reach many tens of metres as it propagates into the shallow seas surrounding distant islands and coastal sites. Such events are relatively frequent in the Pacific Ocean since earthquakes of the required type are common occurrences in the vicinity of the Aleutian Islands and Japan. The semi-permanent isostatic variations of sea level associated with great earthquakes are large enough to be easily observable on tide gauge recordings (e.g. Wyss, 1976a, b; Lagios and Wyss, 1983). RSL changes resulting from such earthquakes may be of the order of 10 cm or more, but such effects are confined to the region in the immediate vicinity of the earthquake itself. The tide gauge data demonstrate that following the initial shock, relative sea level appears to relax back towards its original level over a period of years, as local stresses accumulate in reponse to the driving mechanism of plate tectonics (i.e. thermal convection in the mantle), until the accumulation is eventually released once more by a new earthquake. Much of the best information currently available concerning the dynamics of this earthquake cycle is contained in long time series of RSL change on tide gauge records from the islands of Japan. The effect itself is a good example of those isostatic changes of RSL which are often called *tectonic* in origin. Larger scale tectonic influences on relative sea level–ocean basin shape have been discussed elsewhere (see this vol., Chappell, Ch. 2 and Berryman, Ch. 5).

On somewhat longer timescales, of the order of hours to days, meteorological effects may induce rather substantial changes in relative sea level through the agency of the stress delivered by the wind to the sea surface. Depending upon the local direction of the wind relative to the coast, this stress field may induce either a rise or fall of relative sea level depending on whether the winds are onshore or offshore respectively. Clearly the RSL variations produced by such effects are essentially barotropic, since they are produced by an increase or decrease of the mass of the local water column. Such effects would also, however, be termed eustatic if they were associated with a sufficiently long timescale (climatological) change and aligned in the mean direction of the wind relative to the coast. There is currently a great deal of interest in the oceanographical community in using tide gauge observations of relative sea-level change to infer the strength of the currents through straights and channels as well as the nature of the circulation in the coastal ocean (Csanady, 1982; Thompson, 1981; Noble and Butman, 1979). Of course the most interesting recent application of sea-level data to the problem of inferring the nature of the circulation in the global ocean has been that involving the use of altimetry data from the artificial earth satellites SEASAT and GEOS 3 (Geodynamics Program Office, 1983, 1984). These observing platforms have provided maps of the geoid (the surface on which the gravitational potential is constant and which is coincident with the ocean where there is ocean) of unprecedented

accuracy. These maps are contributing in an important way to advances in both geophysical and oceanographical science (e.g. Stanley, 1979; Rapp, 1979; Wunsch and Gaposhkin, 1980; Wunsch, 1981; Marsh and Martin, 1982; Schutz, Tapley and Shum, 1982; Carter *et al.*, 1986).

On even longer timescales, of the order of years to several years, important variations of relative sea level have been shown to be intimately related to the El Niño–Southern Oscillation (ENSO) phenomenon which is an extremely important source of climate system variability on these timescales (Wyrtki and Nakahoro, 1984). In the ocean the El Niño represents an incursion of warm water from the equatorial zone southward into cooler higher latitude ocean water. In the popular literature ENSO is of course best known for its dramatic effect upon the Chilean anchovy harvest! The ENSO-related RSL fluctuations have ocean basin scale spatial coherence lengths of thousands of kilometres and amplitudes of tens of centimetres. According to Roemmich and Wunsch (1984) the El Niño-like fluctuations of sea level are largely baroclinic rather than barotropic in form and so are not associated with large-scale fluctuations of the local mass of the water column. Rather the relative sea-level variations observed in association with this phenomenon are driven by steric effects, due to the thermal expansion of sea water in response to a changing temperature. An example of the RSL variability associated with ENSO is provided in Figure 3.1. Although the characteristic timescale of ENSO of several years is reasonably long, it is still very significantly shorter than the timescales of hundreds to hundreds of thousands of years upon which most of the ensuing discussion will now focus.

Medium time scale mechanisms

The existence of tide gauge records, many extending as far back into the past as 100 years or more, also provide useful information as to the mechanisms of RSL change which are operative on these extended timescales. On the timescale of 100 years, steric effects also seem to be an important contributor to the global scale secular increase of relative sea level, which appears to be characteristic of this period of earth history. Gornitz *et al.* (1982) have pointed to evidence of a warming of global surface temperature of about 0.4°C during the twentieth century which suggests a sterically induced rate of sea-level rise during this time of about 0.6 mm a^{-1} when interpreted in terms of a model of vertical thermal diffusivity of the ocean. This is sufficient to explain about 50 per cent of the global rate of present-day sea-level rise, inferred on the basis of analyses of the secular variations of relative sea level recorded on a 'global' array of tide gauges, the records of which extend many decades into the past (Barnett, 1983a, b). Examples of the tide gauge records which reveal this

Figure 3.1: Maps of sea-level anomaly for December 1975 and December 1977. Contours show sea-level anomalies in millimetres after removal of the seasonal cycle. These two cases were selected because of the large contrast which they reveal which is characteristic of the El Niño-Southern Oscillation effect

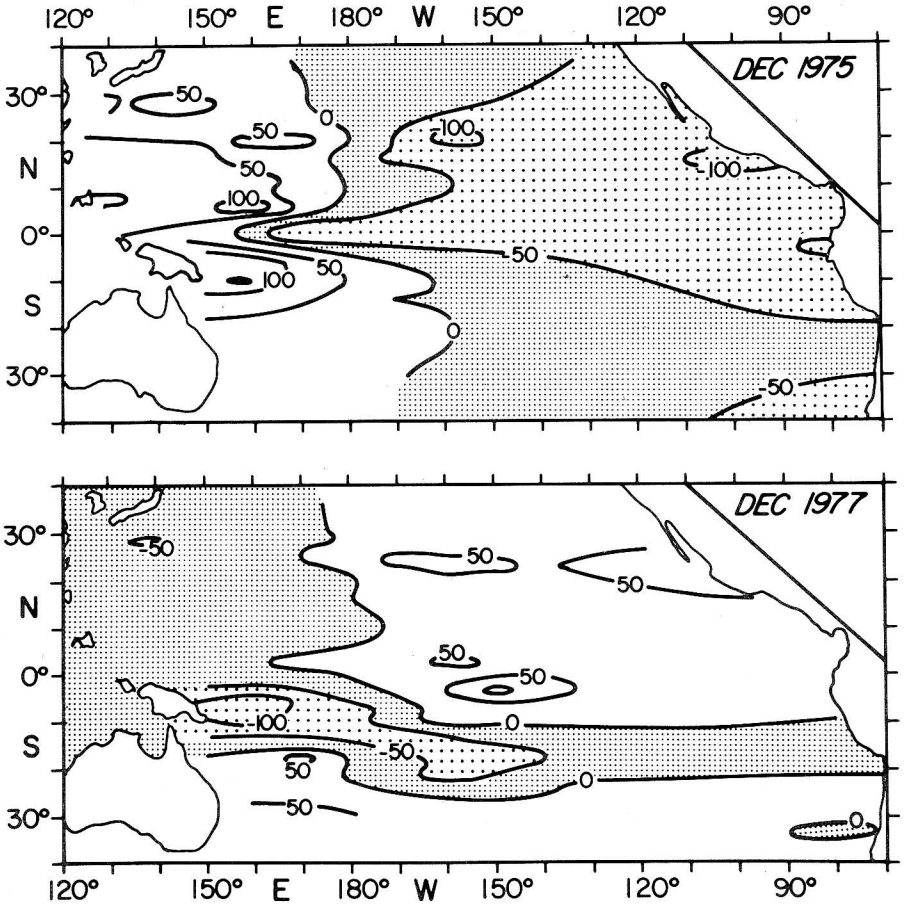

Source: Wyrtki and Nakahara (1984).

secular increase of RSL are provided in Figure 3.2. One of the most hotly debated issues in present-day sea-level research is whether or not the residual non-steric (barotropic) rate of relative sea-level rise of about 0.5 mm a^{-1} is statistically significant. Hansen *et al.* (1981) have suggested that this residual non-steric eustatic contribution could be caused by the melting of continental ice. They further suggest this to be an expected

Figure 3.2: Typical monthly sea-level series for the South Atlanic Bight (Charleston), Mid-Atlantic Bight (Sandy Hook) and Gulf of Maine (Boston), 1950-75

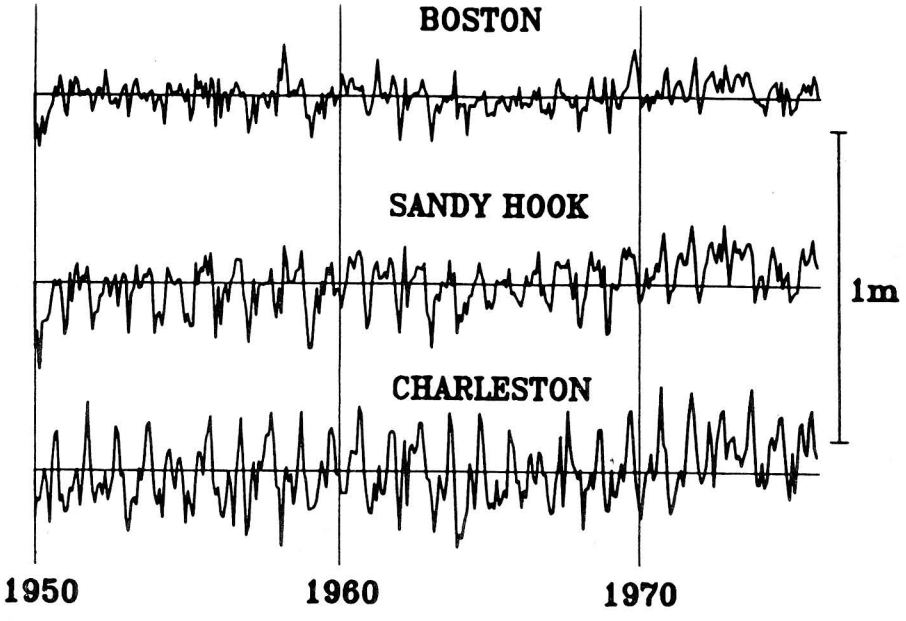

consquence of climate warming due to the increasing atmospheric load of CO_2 and other greenhouse gases, consequent upon the burning of fossil fuels and other side-effects of industrialisation (see Titus, this vol., Ch. 15 for further discussion). Meier (1984) has recently pointed out that although current glaciological evidence suggests that both the Greenland and Antarctic ice masses are stable, the melting back of the small ice sheets and glaciers of the world *is* suggested by the observational evidence. The volume of water released by this process is of an amount which could very nicely account for the increase of water mass in the global ocean, needed to balance the non-steric component of the RSL rise evident on the tide gauge records.

Central to the debate over interpretation of the tide gauge-inferred secular trends of sea level discussed above, is the question of whether or not even longer timescale isostatic processes may be contributing to the observed signals and thereby causing an isostatic signal to be misinterpreted as an eustatic one. This is quite conceivably an extremely serious problem since, as pointed out by Barnett (1983a, b), the global ocean is sampled by the present tide gauge network in a highly non-uniform

fashion. Furthermore, many of the tide gauges from which extremely long records are available, are located in regions, such as along the eastern seaboard of the continental United States, which are known to be strongly influenced by isostatic effects. In the latter region the most important source of ultra long timescale variability of relative sea level, is that associated with the continuing isostatic adjustment of the surface of the solid earth, in reponse to the melting of the huge Laurentide ice sheet. This covered all of Canada and parts of the northern United States until ~ 18,000 BP, by which time it had reached its maximum extent and had begun to retreat, eventually disappearing completely by about 6,500 BP (see Andrews, this vol., Ch. 4). The reason why relative sea level continues to change in response to this cause, so many millennia after the ice sheet had completely disappeared, is the extremely high value of the effective viscosity of the earth's mantle, the viscosity governing the rate at which mantle material flows in the process of restoring the deformed shape of the earth to one of gravitational equilibrium. This process is called *glacial isostatic* adjustment. It is extremely fortunate for geophysical science in general that the earth has conspired to remember the history of relative sea-level variations caused by the melting of such large ice masses. For through careful analysis of these one is able, as will be shown later, to infer the value of the effective viscosity of the mantle. Knowing this number (Peltier, 1980, 1984a, 1985) one is then able to devise an objective test of the validity of the convection hypothesis of continental drift. That this is so makes clear the central place which relative sea-level data have come to play in modern geophysical research.

The way in which the planet remembers the history of deglaciation-induced relative sea-level change is illustrated in Figure 3.3, which shows a flight of raised beaches located in the Richmond Gulf in the southeast corner of Hudson Bay. Each of the horizons (shorelines) visible on the hillside represents a relict beach and therefore a past position of sea level. If one simply measures the height of each of these shorelines above present-day sea level and plots this height as a function of the age of the relict beach, determined by the application of ^{14}C dating to carbonaceous material from systems (e.g. shells) which were open at the time the shoreline was forming, then one obtains a relative sea-level curve (time-depth plot) such as that shown in Figure 3.4. Inspection of this figure shows that relative land emergence has been under way at this location for the last 7,000 years, at a rate which appears to be an exponentially decreasing function of time (see this vol., Andrews, Ch. 4, Sutherland, Ch. 6 and Devoy, Ch. 10 for further discussion of data and techniques). The relaxation time for this process is near 2,000 years and this value can be employed (e.g. Peltier, 1982) to fix the effective viscosity of the mantle beneath Hudson Bay to a value near 10^{21} Pa s. Outside the ice margin, relict beaches are drowned rather than raised, as illustrated by the series of

Figure 3.3: Raised marine shorelines in the Richmond Gulf on the southeastern shore of Hudson Bay

Figure 3.4: Relative sea-level curve obtained by ^{14}C dating of carbonaceous material from the relict shorelines at Richmond Gulf shown on Figure 3.3

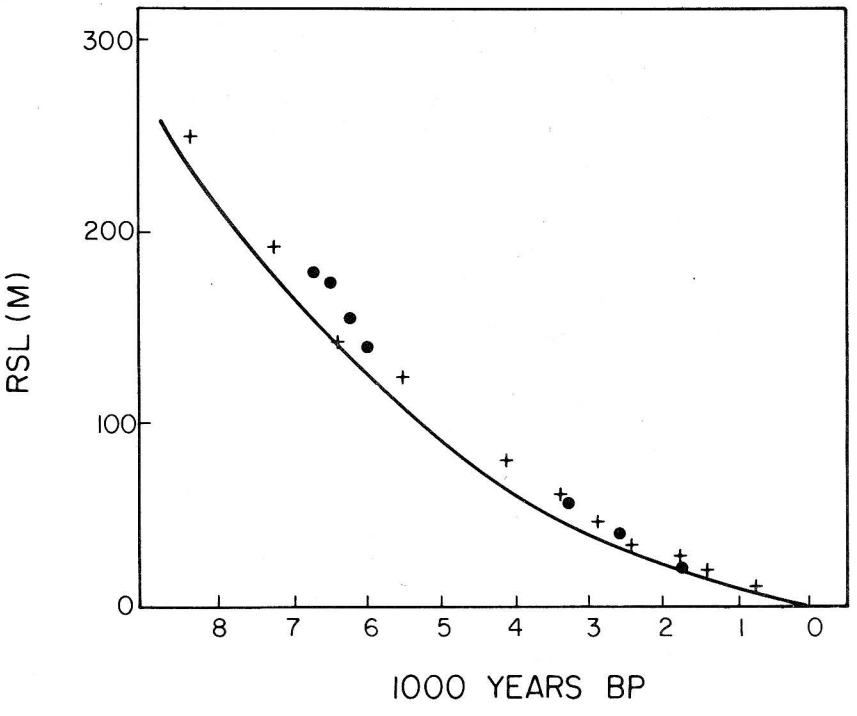

relative sea-level curves from sites along the US east coast shown in Figure 3.5. The reason for this characteristic variation in the RSL signature of glacial isostasy on either side of the ice margin is clear on the basis of a simple conservation of mass argument. At glacial maximum the surface of the earth is depressed under the weight of the ice load by the amount required for the 'Archimedes force' (buoyancy) to balance the weight of the load. This depression of the surface is accommodated by the flow of material out from under the ice sheet into the peripheral region where the surface is elevated above its equilibrium level, producing a forebulge zone (Fig. 3.6). When the ice sheet melts the surface of the earth sinks in the peripheral region as material flows back under the area which was ice covered, causing the surface there to rise out of the sea. Comparing the ^{14}C controlled relative sea-level curves shown on Figure 3.5 with the tide gauge-determined relative sea-level curves shown previously on Figure 3.2, which are for sites along the same coast, brings the problem of the interpretation of RSL data clearly into perspective. What part, if any, of the

Figure 3.5: Relative sea-level curves from four regions along the eastern seaboard of the continental United States

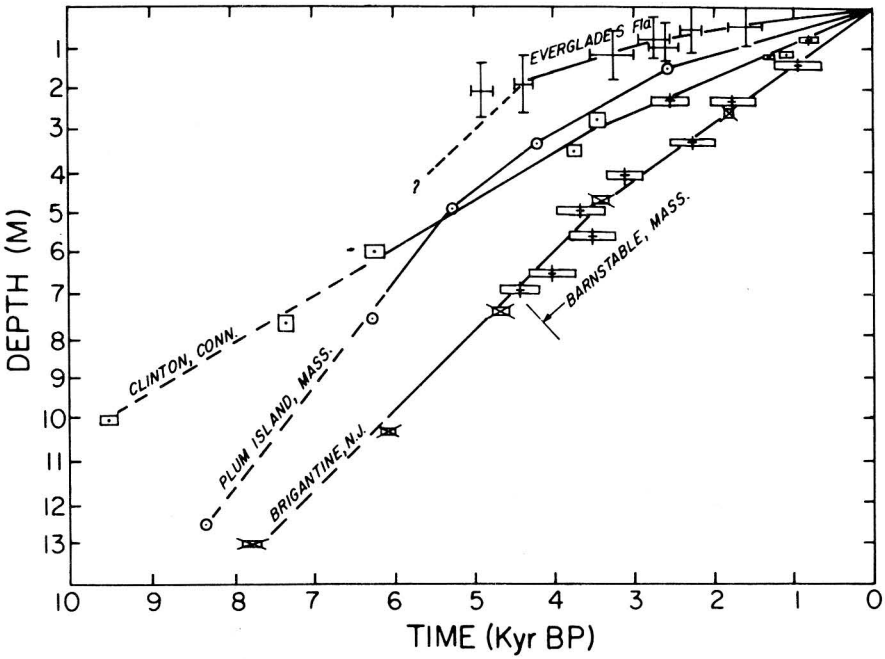

Source: Modified from Bloom (1967).

secular change seen on the tide gauges is not explicable in terms of the glacial isostatic adjustment effect? If such a eustatic component exists, is it entirely explicable as a steric effect, or must we invoke a change in ocean mass to understand it? In the next section of this chapter the theory of glacial isostasy will be used to illustrate, by a specific example, the way in which questions such as this may be objectively addressed.

Long timescale mechanisms

Before doing so, however, it will be useful to consider mechanisms of sea-level change which operate on timescales longer still than the roughly 10 ka timescale over which the glacial isostatic adjustment process has contributed dominantly to the record of RSL variability. On a timescale of 100 ka-1 Ma, the dominant contributor to the RSL record has been the

Figure 3.6: Model showing the effects of glacio-isostatic ice mass load on a land surface. Isostatic depression of the land surface A–B increases with ice load so that greater depression occurs towards the centre of an ice mass (h_1) than at the margin (h_2)

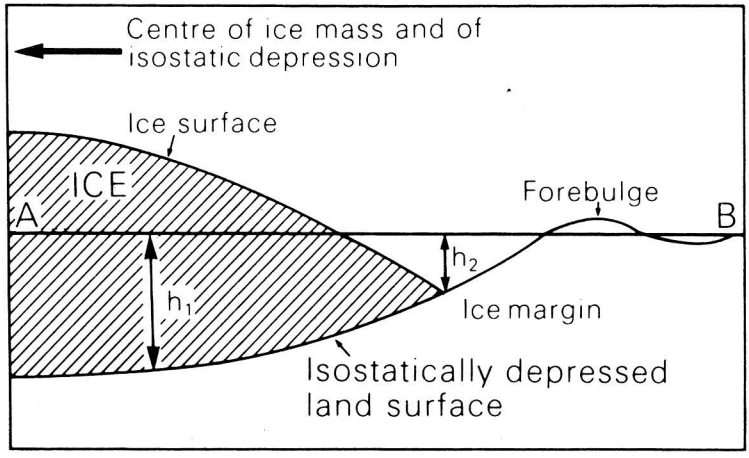

Source: Lowe and Walker (1984).

continuous process of accumulation and disintegration of large ice sheets, such as that which last covered Canada 18,000 years ago. In fact this ice sheet, along with its apparently inevitable Fennoscandian companion centred on the Gulf of Bothnia and a third sheet centred on West Antarctica, have been appearing and disappearing at regular 100 ka intervals for at least the past 700,000 years of earth history. Since the mass of ice bound in these complexes was extremely large when they were at their maximum extents, approximately 3.5×10^{19} kg in total, their growth caused a global eustatic fall of sea level (*glacio-eustasy*) of ~110 m, although opinions vary on this value (Bloom, 1983). Our knowledge that this has been the case derives from $\delta^{18}0$ vs. depth data obtained from sedimentary cores drilled from the floors of the major ocean basins, at sites well removed from the continental margins where turbidity current effects continually disturb the sedimentary record. The number $\delta^{18}0$ is simply a measure of the concentration of the heavy isotope of oxygen ($^{18}0$) relative to the more abundant light isotope ($^{16}0$). Examples of such data from four typical sedimentary cores are shown in Figure 3.7, using data from Shackleton and Opdyke (1973, 1976) and Imbrie *et al.* (1973). The importance of these data derives from the fact that $\delta^{18}0$ in the sediment is a direct measure of the amount of continental ice which exists in the climate system at the time of

Figure 3.7: Four typical $\delta^{18}0$ vs depth series obtained from long DSDP cores in three different oceans. M + B = Brunhes–Matuyama boundary, at 730,000 ± 10,000 ka

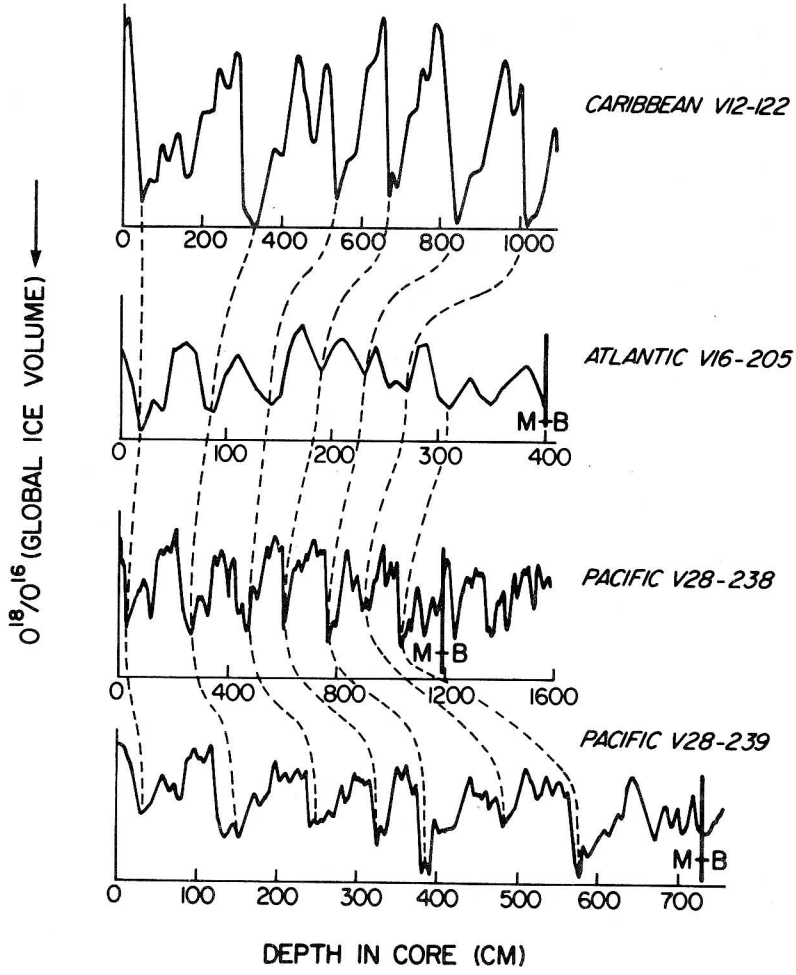

sediment deposition. This is because the process of evaporation of water at the sea surface, which provides the fuel through which later precipitation induces ice sheet growth, is a process which fractionates mass. Since the light isotope evaporates preferentially over the heavy, the precipitation which feeds ice sheets is always isotopically light, which is to say that it has lower $\delta^{18}0$ than normal sea water. Therefore, when ice accumulates on land this leads to an irreversible increase of the $\delta^{18}0$ of sea water, which is communicated to the organisms (e.g. foraminifera, coccoliths) whose shells

(upon their death) contribute to the sediment which accumulates on the sea floor. When we later measure the $\delta^{18}0$ of the shells contained in the sediment at some depth in the core, corresponding to some time in the past, we are therefore able to infer how much ice must have been present on the continental surface at that time. Although we obviously cannot infer from these data where the ice was located, we can deduce, on the basis of the observation that indications of the presence of ice sheets (moraines, erratics, glacial striae) are noticeably absent in regions well removed from Laurentia and Fennoscandia, that the ice sheets must have continually reoccupied these same locations.

In order to make quantitative use of $\delta^{18}0$ data such as that shown in Figure 3.7, we must be able to calibrate the record so that we can quantitatively infer the volume of continental ice from the observed $\delta^{18}0$ measurement. This can be done relatively simply by using the known volumes of the Greenland and Antarctic ice sheets in conjunction with measurements of their oxygen isotopic signatures. We must also find a way to assign a specific age to a specific depth in each core. Clearly the same age will not correspond to the same depth in each core because the rate of sedimentation is a strong function of location on the ocean floor. For sedimentary cores which are sufficiently long, this problem may be rather elegantly solved by finding the depth in the core corresponding to the first horizon below which the remnant magnetisation of the sediments has the opposite direction from that above. This horizon corresponds to the time (down core) of the last reversal of the earth's magnetic field and is referred to as the Brunhes–Matuyama boundary. Since this reversal occurred 730,000 ± 10,000 BP (Cox and Dalrymple, 1967), if we can find the depth of the horizon corresponding to it in the core we can, assuming that the sedimentation rate has remained constant over the time spanned by the core, translate each specific depth into a specific time. Imbrie *et al.* (1984) have attempted to produce a 'best' $\delta^{18}0$ chronology from these data by stacking the time series from a number of such cores to discriminate against features which are not consistent from core to core. They have called the resulting record SPECMAP (Fig. 3.8). Obvious by inspection of the power spectrum (Fig. 3.8b) is the fact, first noted by Hays *et al.* (1976), that the dominant variability in the $\delta^{18}0$ data occurs at the periods of 100 ka (over 65 per cent of the variance), 41 ka, 23 ka and 19 ka. Since these are rather precisely the period of variation of the eccentricity of the earth's orbit around the Sun, the period of variation of the tilt of the spin axis with respect to the ecliptic and the dominant periods of the precession of the equinoxes, these data have been construed as verifying the validity of the Milankovitch (1941) theory of palaeoclimatic change. The largest (eustatic) changes in relative sea level of all, therefore, appear to be driven by the small changes of the effective intensity of (summer) solar insolation, caused by equally small changes in the values of the parameters which

Figure 3.8: (a) the SPECMAP time series of Imbrie *et al.* (1984) and (b) its power spectrum

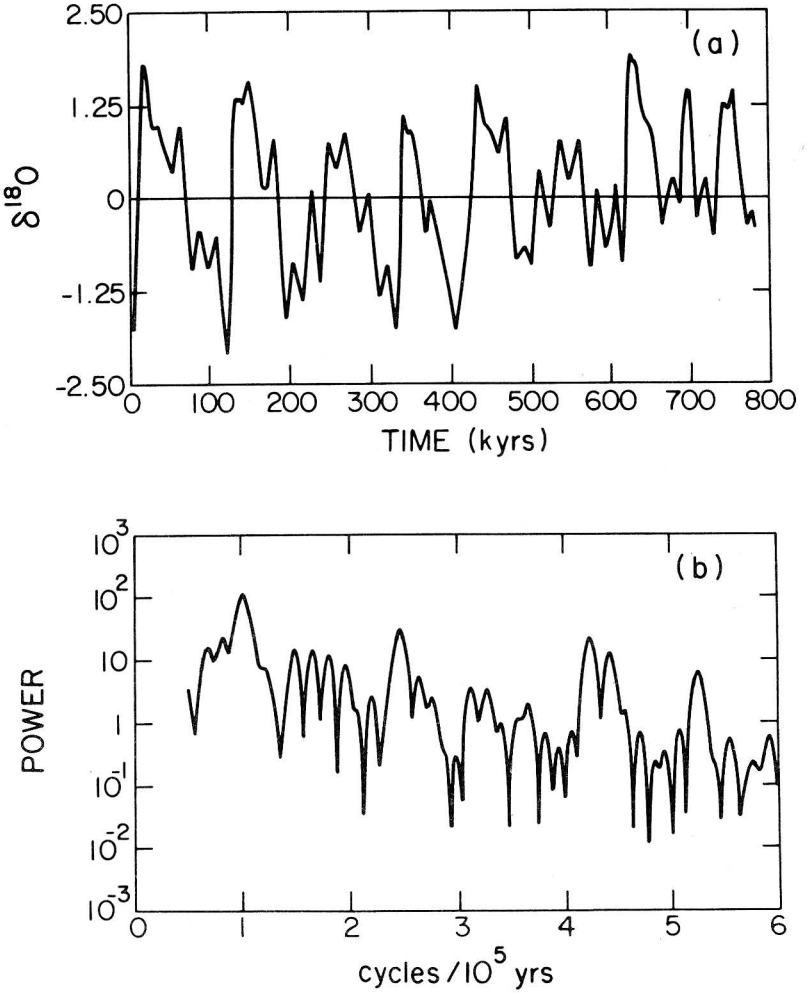

govern the geometry of the earth's orbit around the Sun. Much recent effort has been invested in explaining the detailed physical processes through which the astronomical input is translated into the ice volume fluctuations revealed by the $\delta^{18}0$ data (e.g. Peltier, 1982; Peltier and Hyde, 1984; Hyde and Peltier, 1985).

The extremely large amplitude glacio-eustatic variation of global sea level which accompanies the 'ice age cycle' suggests the operation of a

further important mechanism of relative sea-level change. In any analysis of relative sea-level data during times of active ice sheet disintegration at sites near the glaciated regions, or at any time from sites well removed from the ice sheets, there will be an important contribution to the observed variation of relative sea level resulting from the direct effect of the water load applied to the ocean basins as the ice sheets melt. This water load will in turn induce its own deformation of the solid earth. This process is called *hydro-isostasy* (Bloom, 1967). It should be clear that as the earth deforms physically due to loads associated with ice sheet melting and ocean basin filling, this deformation will cause continuous changes in the gravitational potential field of the planet. This will require continuous redistribution of mass among and within the ocean basins in order to ensure that the surface of the sea (the ocean geoid) remains an equipotential surface. The actual history of relative sea-level change which is observed at any particular location on the earth's surface is therefore the consequence of a complex interaction, through the intermediary of the gravitational field, between the aquasphere, the cryosphere and the solid earth. This complex of interactions is illustrated by the schematic feedback loops shown in Figure 3.9. Over the past decade it has proved possible to develop a detailed mathematical model capable of accurate prediction of postglacial variations of relative sea level, including both glacial isostasy, hydro-isostasy and the full effects of the mutual gravitational attraction acting between the ice and sea water in a self consistent way. The next section of this chapter will now present a few of the detailed characteristics of this model, together with a discussion of the geophysical and oceanographical data which it has been shown to reconcile. Further, an application of the model is made in addressing the specific question raised earlier in this section, namely, the origin of the secular trend of rising relative sea level which seems to be characteristic of the last hundred years of earth history. It is hoped that by more sharply focusing the discussion to follow in this way the reader will be able to see the wealth of information that is contained in relative sea-level and associated data much more clearly than would be possible with further general commentary.

THE GLOBAL MODEL OF GLACIAL ISOSTASY AND POSTGLACIAL RELATIVE SEA-LEVEL CHANGE

The mathematical structure of the global model of glacial isostatic adjustment has been reviewed recently in Peltier (1982) to which the interested reader is referred for details. In this model the planetary interior is assumed to be radially stratified, with an elastic structure fixed by observations of the frequencies of the elastic gravitational modes of free oscillation, as described for example by Gilbert and Dziewonski (1975). The rheology of

Figure 3.9: Schematic diagram illustrating the interactions among ice loads, water loads, and the deformable earth: (A) The weight of the ice deforms the earth and (B) the ice mass attracts the water. (C) The transfer of matter within the earth distorts the geoid. Similarly, (D) the weight of the meltwater depresses the earth differentially and (E) more water flows into this depression, increasing the water load and (F) causing added deformation of the ocean floor. These processes are interrelated as indicated in (G), and all are included in the numerical model

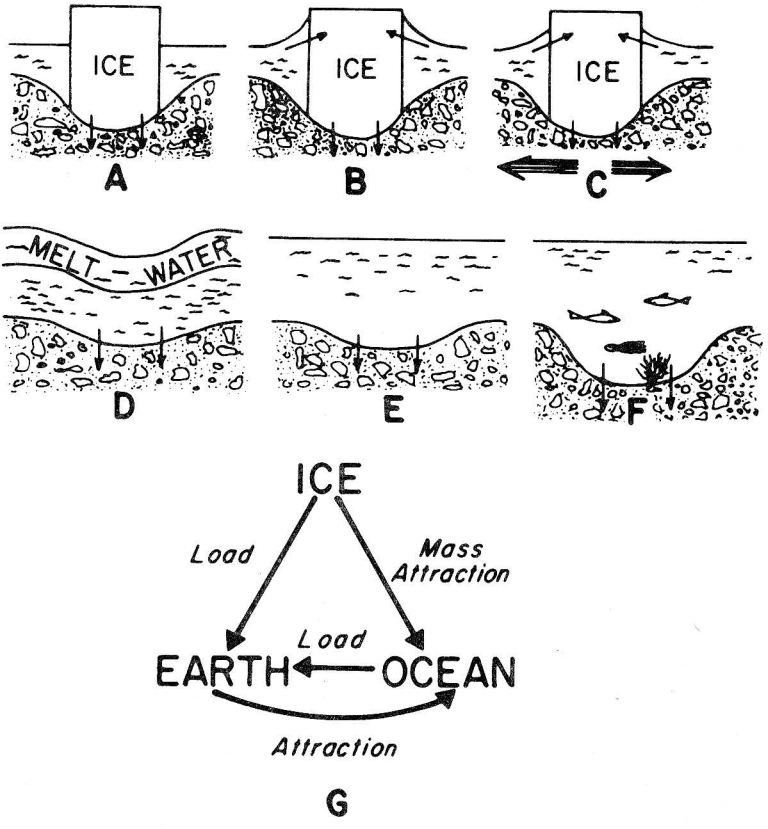

Source: Clark *et al.* (1978).

the interior is assumed to be linearly viscoelastic and either of the 'Maxwell' or 'Burger's' body type. In the former the initial response of the material to an applied shear stress is Hookean elastic, whilst the final response is Newtonian viscous and governed by a viscosity ν_1 which is a function only of radial position r within the planet. The Burger's body differs from the Maxwell analogue in that it includes a transient as well as a

Newtonian steady state component in its viscosity spectrum (Peltier *et al.*, 1981; Peltier 1982, 1984a, 1985a, b). This requires specification of a second viscosity $\nu_2(r)$ to complete the description of the rheology. As demonstrated explicitly in Peltier (1985a), however, even if transient rheology is important in the glacial isostatic adjustment process, only models with large elastic defect are capable of simultaneously reconciling all the data. In this large defect limit the transient Burger's body model behaves as a Maxwell model with a new effective viscosity $\nu_{eff}(r) = \nu_1(r)\nu_2(r)/(\nu_1(r) + \nu_2(r))$. When we fit a Maxwell model to RSL data such as that shown in Figures 3.4 and 3.5 we are free to vary only the one parameter $\nu_{eff}(r)$ to achieve the fit.

In the actual prediction of such RSL variations what one does is to assume a melting history for all of the surface ice loads which exist at glacial maximum. A computation is then made, in a gravitationally self-consistent fashion, including the full effects of both glacial and hydro-isostasy and the ice-water attraction, of the manner in which the meltwater must be distributed over the global ocean. This is done in order to ensure that the instantaneous surface of the new ocean is maintained as an equipotential surface at all times as the system evolves. This process requires inversion of an integral equation at every instant during, and subsequent to, the deglaciation event, and results in a direct prediction of the time dependent separation of the geoid and the surface of the solid earth at any point on the earth's surface where ocean and land meet. In the model, the geography of the oceans and continents is realistically described and the integral equation is inverted using a finite element discretisation of the surface. Further, a Green's function formalism is employed to describe the gravitational interactions between the aquasphere, cryosphere and solid earth components of the model, which are fundamental to the determination of sea-level change.

It is rather fortunate that it is possible to make reasonably accurate *a priori* estimates of the deglaciation histories of each of the three main ice-covered regions (Laurentia, Fennoscandia, and West Antarctica) subsequent to 18,000 BP. Without this information we would not be in any position to implement the relative sea-level model discussed above! Peltier and Andrews (1976) have described the way in which ^{14}C age controlled terminal moraine data can be combined with worldwide observations of RSL and ice physical–mechanical information to develop first order models of the glacial chronology. Their initial model, called ICE-1, has since been improved by Wu and Peltier (1983) who have called the new model ICE-2 (Fig. 3.10). This shows three time slices through the ice sheet topography for both the Laurentian and Fennoscandian regions. The initial problem for RSL prediction takes this deglaciation history as input to the model and, in conjunction with an assumed model of the planet's radial viscoelastic structure, produces as output a prediction of the RSL variation which should be

Figure 3.10: Three time slices through the ICE-2 melting chronologies for Laurentia (Canada), and Fennoscandia. The ice thickness contours are in metres

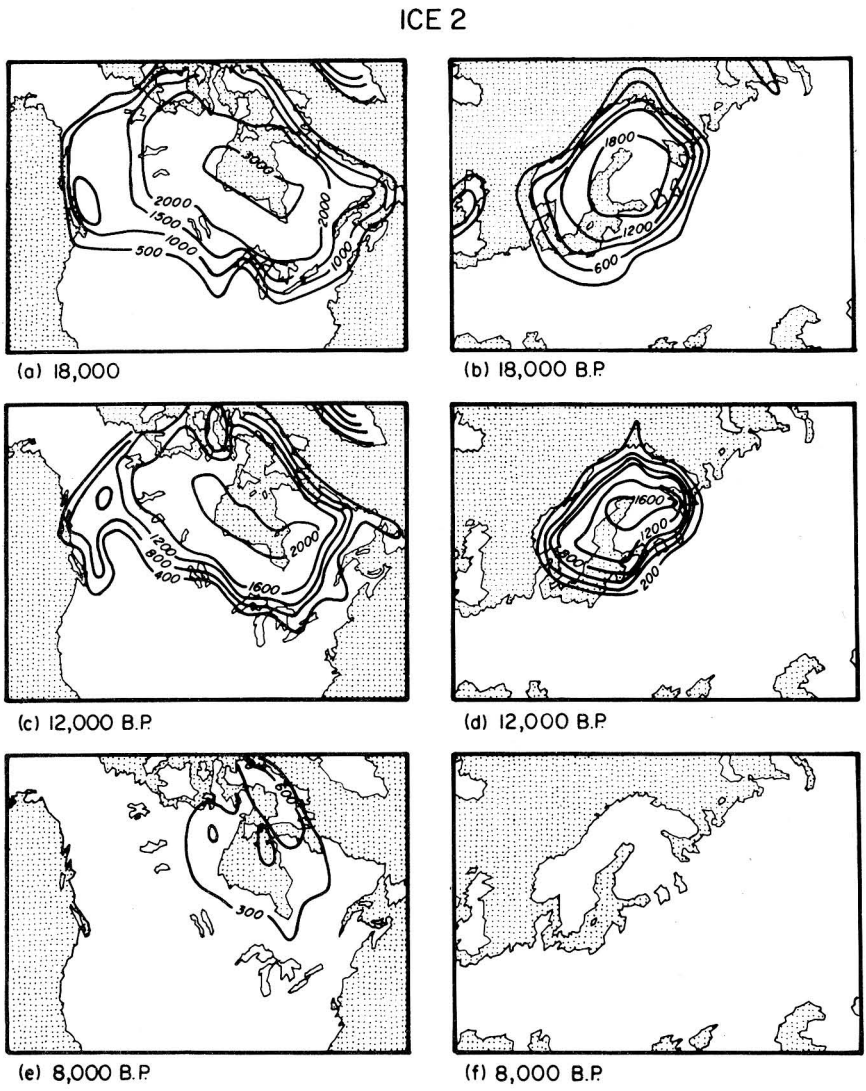

observed at any site on the earth which might be of interest. In fact the primary output of the model consists of a sequence of maps, such as those shown on Figure 3.11, for four sample times within and subsequent to deglaciation. These maps show the increase or decrease of the local bathymetry of the ocean which has occurred by the time shown on each plate. This includes the combined effects of the glacial isostatic and hydro-isostatic

Figure 3.11: Four time slices through a typical solution of the sea-level equation. The relative sea-level rise is contoured in metres. Details of the model employed to make this prediction are provided in the text

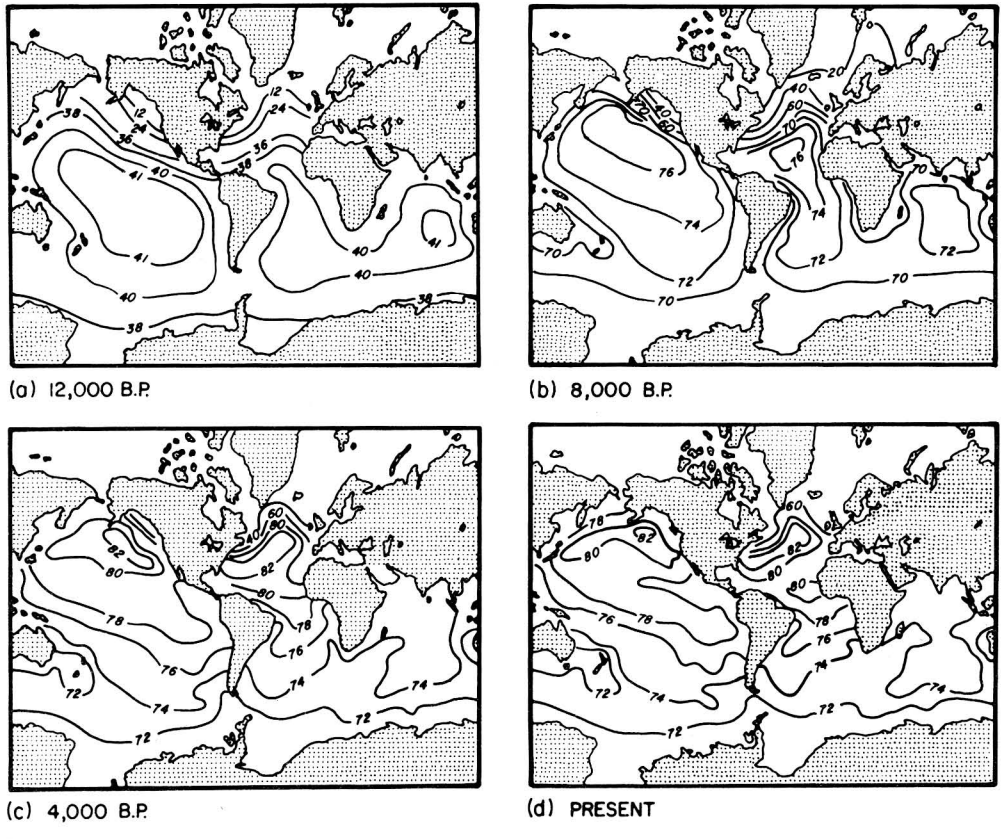

displacement of the surface of the solid earth, as well as the eustatic sea-level variation forced by the filling of the ocean basins by the meltwater produced in glacial decay. It also includes the full effects of the geoidal deformation associated with the redistribution of surface load and with the load-induced deformation of the solid earth. Inspection of the four plates of Figure 3.11 demonstrates that the increase of ocean bathymetry caused by ice sheet melting is a highly non-uniform function of position in the global ocean. There therefore does not exist a single 'eustatic curve' which could be used to characterise the effect of increasing water mass upon relative sea level at all locations remote from the main ice sheet centres.

Prior to the development of the model described here, which is based upon the theoretical description of glacial isostasy first advanced in Peltier (1974) and further refined in a number of subsequent papers (Peltier, 1976; Peltier and Andrews, 1976; Farrell and Clark, 1976; Peltier *et al.*, 1978; Clark *et al.*, 1978; Peltier, 1982; Wu and Peltier, 1983), it was generally believed that such a universal curve did exist and could be used to correct all relative sea-level data for the effect of glacial eustasy (e.g. Shepard, 1963). This was at least partly responsible for an important controversy which arose concerning the explanation of emerged Holocene beaches, which are found in a wide variety of locations at sites remote from the main glaciation centres. Several scientists had expressed opinions to the effect that these beaches were formed when postglacial eustatic sea levels were higher than they are at present and, therefore, inferred the occurrence of important climatic changes (e.g. Schofield, 1964; Gill, 1965; Fairbridge, 1976). Others disputed this contention and suggested either that the observed beaches were much older than Holocene in age, or were emerged as a consequence of tectonic activity, or simply the product of intense but infrequent storms (Shepard, 1963; Jelgersma, 1966; Bloom, 1970). The gravitationally self-consistent model of postglacial relative sea-level change has settled this controversy. It demonstrates that the emergence of shorelines at locations remote from ice sheet influence is an entirely expected consequence of the viscoelastic adjustment of the earth, in response to the changing ice and water load on its surface and the geoidal deformation which is thereby produced. This fact is demonstrated in Figure 3.12 which shows the surface of the earth divided into a number of zones, in each of which the variation of relative sea level is of a single characteristic form. The model which produced this result is described in detail in Wu and Peltier (1983, Figure 24). The earth is assumed to possess an elastic structure identical to that of model 1066B of Gilbert and Dziewonski (1975), the lithosphere is assumed to be 120.7 km thick and the mantle to have a constant viscosity of 10^{21} Pa s from the base of the lithosphere to the core-mantle boundary. The deglaciation history is essentially the ICE-2 model of Wu and Peltier (1983), although the melting from West Antarctica was neglected. In Zone I, which comprises the ice-covered regions, the

Figure 3.12: Zone boundaries separating the surface of the earth into six regions, in each of which the history of relative sea-level change since deglaciation has a characteristic form (see also Clark *et al.*, 1978)

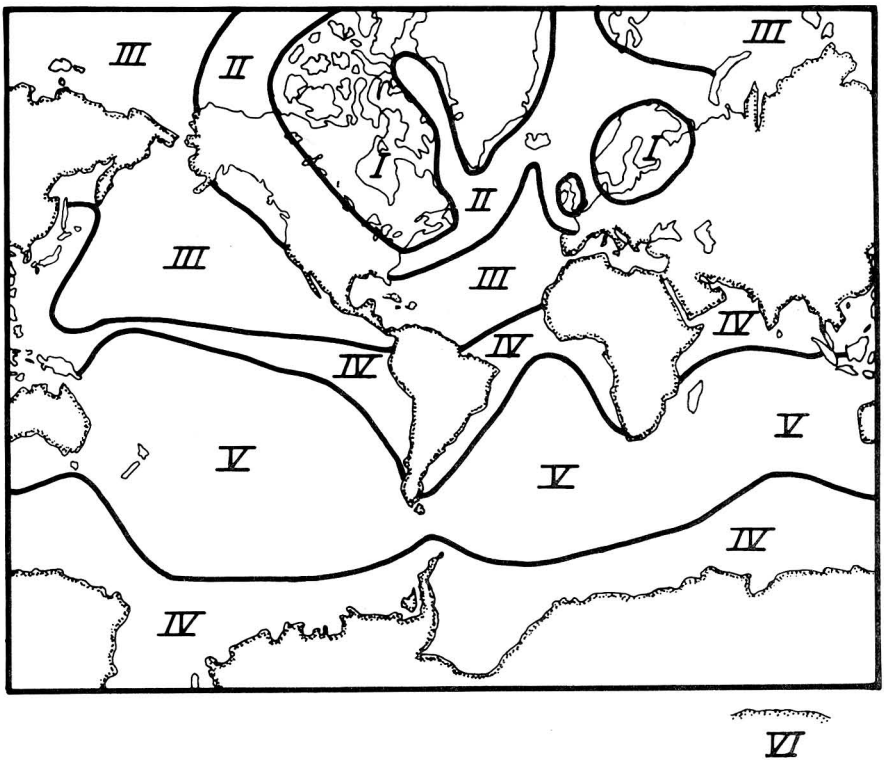

relative sea-level curves all display monotonic emergence, while in the peripheral bulge region of Zone II the predicted RSL signature is one of monotonic submergence. For this model Zone III is one in which raised beaches appear some finite time after the cessation of glacial decay, while in Zone IV the model predicts monotonic submergence. In Zone V raised beaches form immediately after the cessation of melting whilst in Zone VI, which comprises all continental shorelines removed from ice sheet influence, raised beaches are produced subsequent to glacial decay by the deformation associated with the offshore water load. Of course the existence of the zones and the locations of the boundaries separating them are a strong function of the earth and deglaciation models and can therefore be employed to discriminate between them.

The brief summary of the model presented here should be sufficient to demonstrate that when the full effects of glacial isostasy, hydro-isostasy

and geoid deformation are included, the model is able fully to account for the occurrence of raised beaches distant from the effects of ice sheet development. There is no need to invoke further eustatic or tectonic contributions to the sea-level record subsequent to completion of the last deglaciation event, which ended ~6500 BP. The remaining sections of this chapter describe a sequence of detailed comparisons of the predictions of this model with specific relative sea-level curves and with several other geophysical and astronomical observations which are also explicable as representing various signatures of the planet's response to the Pleistocene glacial cycle.

POSTGLACIAL VARIATIONS OF RELATIVE SEA LEVEL AND RELATED EFFECTS

Figure 3.13 shows typical examples of observed and predicted relative sea-level variations at six locations on the North American continent (see Devoy, this vol., Ch. 10, for discussion of the sea-level record). Three occur at sites which were once ice covered (Fig. 3.13a, b and c) and three at locations along the east coast of the continental United States in the peripheral region of monotonic subsidence (Fig. 3.13d, e and f). The earth model employed to make these predictions has the elastic structure 1066B of Gilbert and Dziewonski (1975), an upper mantle viscosity of 10^{21} Pa s and a lower mantle viscosity beneath 670 km depth of 2×10^{21} Pa s. On each plate comparisons are shown for three different models which differ from one another only in terms of their lithospheric thicknesses. Inspection of these comparisons shows that the relative sea-level data at sites inside the ice margin are reasonably well fitted by the theoretical model and that the RSL variations at these sites are rather insensitive to changes of lithospheric thickness. This is entirely expected as the spatial scale of the Laurentian ice sheet (Fig. 3.10) is so large that the lithosphere is transparent to the response at locations which were once under the ice sheet centre. At sites in the peripheral region, on the other hand, the response is extremely sensitive to lithospheric thickness, as the deformation at such sites is significantly affected by relatively short horizontal wavelengths, which 'see the lithosphere clearly'. In Peltier (1984b) this sensitivity was first exploited to measure lithospheric thickness and a relatively high value in excess of 200 km was obtained. As reviewed in Peltier (1982), the totality of ^{14}C controlled RSL data also require an almost uniform profile of mantle viscosity, with little variation between the upper and lower mantles. Weertman (1978) has commented upon this result from the point of view of theoretical ideas concerning the microphysical basis of solid state creep in the earth. He has suggested that it might be taken to imply that the relaxation of the lower mantle, which occurs in postglacial rebound, is

Figure 3.13: Example comparisons of observed and predicted relative sea-level histories at six sites on the North American continent as a function of lithospheric thickness in a model with 1066B elastic structure, upper mantle viscosity of 10^{21} Pa s and lower mantle viscosity of 2×10^{21} Pa s. The first three sites (a, Churchill; b, Ottawa Islands; c, Southampton Islands) were ice covered whereas the last three (d, N.Y. City; e, Brigantine; f, Delaware) were beyond the ice margin on the US east coast

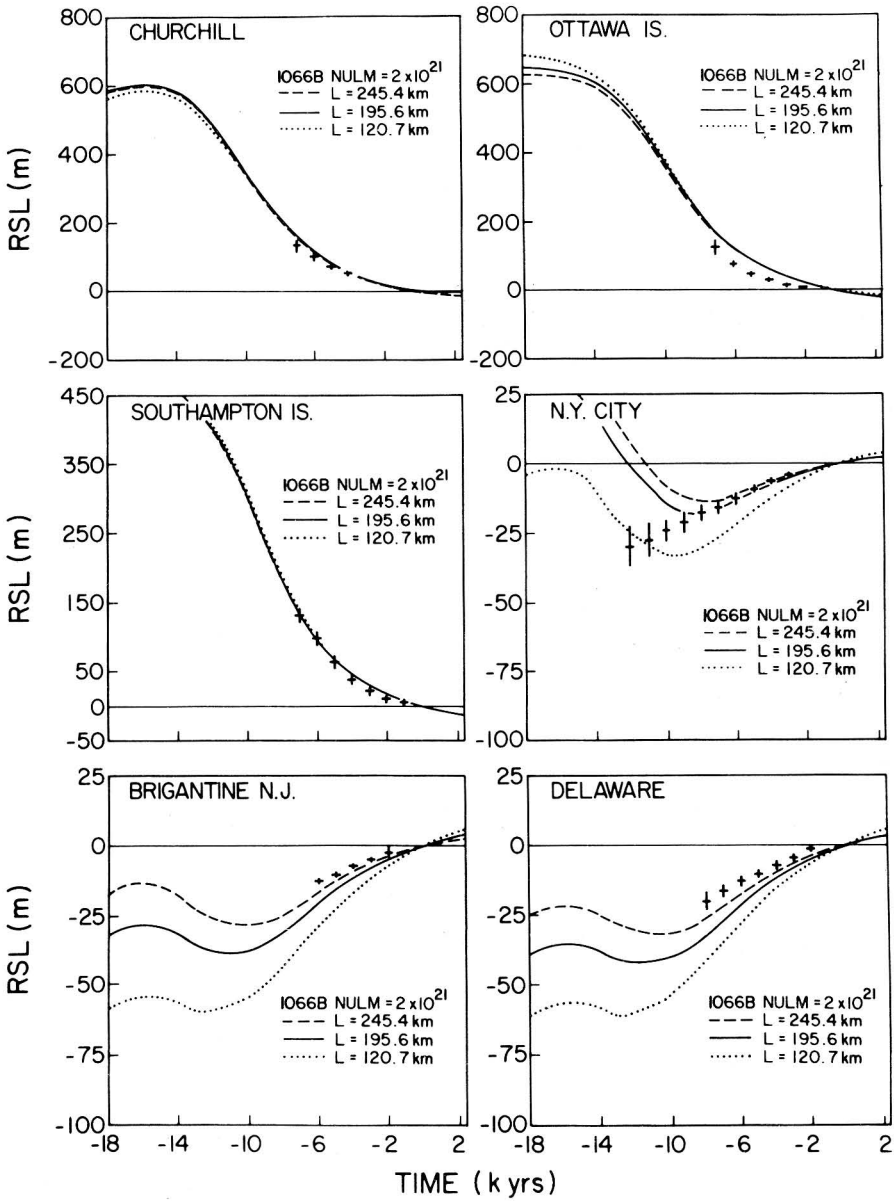

controlled by transient creep rather than the steady state creep which is assumed in the Maxwell analogue. This possibility may be tested using the simple Burger's body rheology derived in Peltier *et al.* (1981). It includes the transient component of the response via a single Debye peak governed by two additional physical constants. As previously mentioned, however, an analysis of the asymptotic properties of the Burger's body rheology demonstrates that when the elastic defect is large, and the short and long timescale viscosities sufficiently different, the Burger body rheology again behaves like a Maxwell solid, but with a viscosity equal to that which governs the short timescale transient response. Under these circumstances the lower mantle viscosity, inferred by analysis of rebound data based upon the Maxwell analogue, would be the transient viscosity as originally suggested by Weertman (1978).

The free air gravity anomaly over centres of postglacial rebound

Figure 3.14 shows maps of the free air gravity anomalies over the present-day centres of postglacial rebound in Laurentia (Fig. 3.14a) and Fenno-scandia (Fig. 3.14b) respectively. Comparison of these maps with those for ice thickness at glacial maximum (Fig. 3.10) demonstrates a high degree of correlation between these two fields and provides strong support for the hypothesis that the observed free air anomalies are to be interpreted as measures of the currently existing degree of isostatic disequilibrium in these two regions. Figure 3.15 shows a comparison of observed and predicted

Figure 3.14: Observed free air gravity anomalies in milligals for (a) Laurentia and (b) Fennoscandia

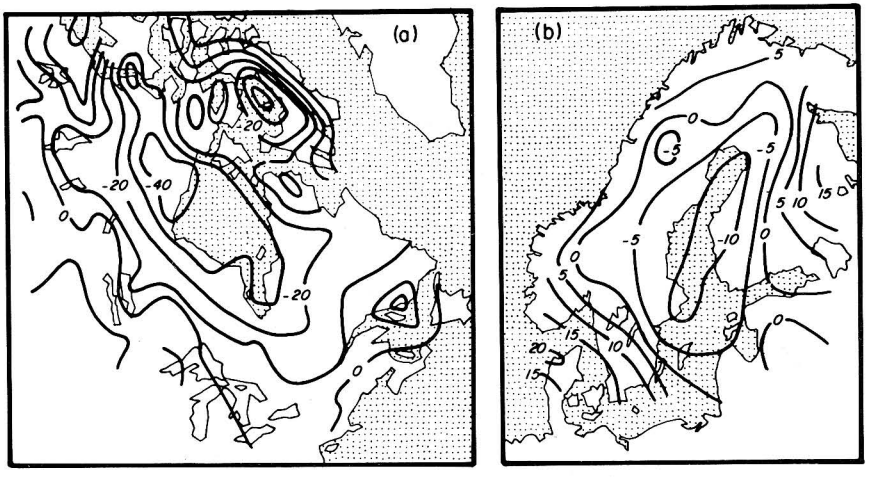

Figure 3.15: Observed (stippled) and predicted peak present-day free air gravity anomalies for Laurentia and Fennoscandia in models with a fixed upper mantle viscosity of 10^{21} Pa s as a function of the lower mantle viscosity. The predictions denoted □ are for a model with uniform mantle density (an adiabatic model), △ is for a model with a 6.2 per cent increase of density below 670 km depth, + is for a model with a 12.4 per cent increase at 670 km depth, while ▽ is for a model with a 6.2 per cent increase at 670 km and a 3.8 per cent increase at 420 km. The predictions denoted × and ○ are respectively for the seismically realistic models 1066B and PREM, in which the entire radial variation of density is treated as non-adiabatic

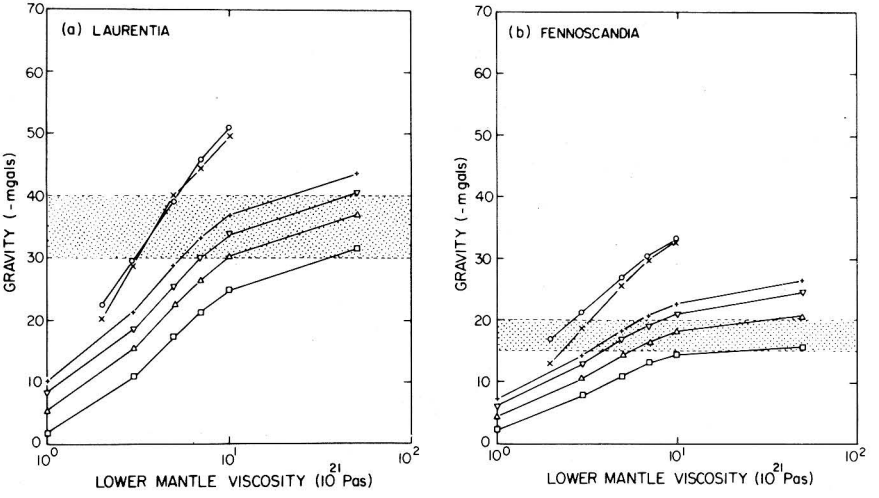

present-day peak free air anomalies for Laurentia and Fennoscandia, for a number of earth models having fixed lithospheric thickness of 120.7 km and an upper mantle viscosity of 10^{21} Pa s, as required by the sea-level data discussed previously. The earth models employed differ from one another only in terms of their elastic structures, and lower mantle viscosity is varied through the same sequence of values for all models. As described in the figure caption, four of the models are flat homogeneous layered approximations to the 1066B elastic structure. These have either 1 or 2 internal discontinuities of elastic parameters within the mantle at 420 km and/or 670 km depth, corresponding to the depths of the Olivine–Spinel and Spinel–Post Spinel phase boundary horizons. The remaining two curves are for the seismically realistic models 1066B of Gilbert and Dziewonski (1975) and PREM of Dziewonski and Anderson (1981). In these models all of the radial variation of density is treated as though it were non-adiabatic. Inspection of these results shows that to fit the observed free air gravity anomalies with a model with weak radial variation of viscosity, requires the presence in the model of significant internal buoyancy,

associated with a density structure which behaves non-adiabatically on the timescales of glacial rebound. This requires at least that the density variations across the phase boundaries at 420 and 670 km depth behave in this fashion, which is possible only to the extent that these transitions may be considered univariant (e.g. O'Connell, 1976; Mareschal and Gangi, 1977). Although such behaviour is not inconceivable, it may also prove possible to reconcile these data by appealing to other physical effects. This is clearly an extremely important issue in so far as the problem of mantle convection is concerned (Peltier, 1985b).

Pleistocene deglaciation and earth rotation

From about 1900 AD until 1982 the location of the earth's north pole of rotation was carefully monitored by the International Latitude Service (ILS), using a global network of photo-zenith tube equipped observatories. Since 1982 this observing system has been replaced by the much more accurate VLBI-based network of the IRIS earth orientation monitoring system, which routinely determines the pole position at 5-day intervals with a verified accuracy of 2 milliseconds of arc (Carter and Robertson, 1986). Although these new data will quickly replace the old as the industry standard, the duration of the time series is still sufficiently short that the ILS data remain the best source of information on the secular motion of the pole. These data are shown in Figure 3.16 as x and y components of the displacement relative to the axes shown on the inset polar projection. The origin of the co-ordinate system corresponds to the Conventional International Origin or CIO. Inspection of these data, which are based upon the reduction by Vincent and Yumi (1969, 1970), demonstrates that the dominant oscillatory signal, which consists of a 7-year periodic beat generated by the interference between the 14-month Chandler and 12-month Annual wobbles, is superimposed upon a secular drift at the rate of $0.95° \pm .15°$ Ma^{-1} towards Hudson Bay. The direction of this drift is shown by the arrow on the inset polar projection (Fig. 3.16).

In 1952 Munk and Revelle interpreted this observed secular drift of the rotation pole as requiring some present-day variation of surface mass load, and suggested that the cause of the apparently required variation might be found in melting of ice on Greenland and/or Antarctica. Their inference that such an effect was required to explain the data was, however, based upon a dynamical model. Here it was assumed that the earth could be treated as an homogeneous viscoelastic sphere, in so far as its rotational response to surface loading was concerned. To the extent that this approximation is valid the inference of Munk and Revelle is completely correct, since the theory then shows that the pole must be fixed at any instant of time in which the surface load is steady. As first demonstrated in Peltier

Figure 3.16: Polar motion data from the ILS records 1900-77, with the displacement shown as x and y components relative to a co-ordinate system with origin at the CIO (conventional international origin). The dominant oscillatory signal is due to the interference between the 12 month Annual and 14 month Chandler wobbles. This is superimposed upon a secular drift in the direction denoted by the arrow on the inset polar projection, where the locations of the major ice masses at 18 ka BP are shown stippled. This secular drift has been shown to be exactly that which is expected due to the disintegration of the Northern Hemisphere ice sheets

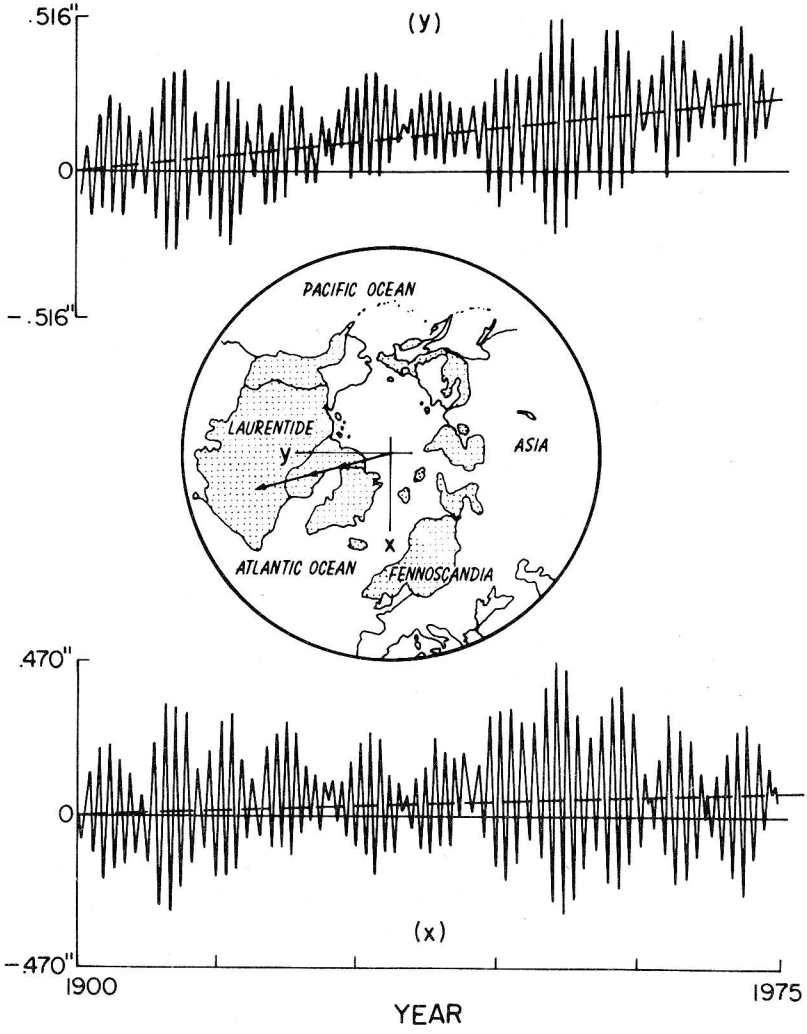

(1982) this holds true for homogeneous earth models, since in this limit the isostatic adjustment and rotational contributions to the rotational forcing counteract one another exactly. For radially stratified models, however, the dynamical symmetry which underlies this cancellation is broken and polar wander can occur even at a time when the surface load is steady. It therefore becomes plausible that the secular drift of the rotation pole shown on Figure 3.16, could simply be an effect due to the influence of planetary deglaciation, which began at ~ 18,000 BP and ended at about 7,000 BP. In Peltier (1982), Peltier and Wu (1983), Wu and Peltier (1984) and Peltier (1984) it was demonstrated that both the observed rate and direction of polar drift are just those to be expected if the earth has the viscoelastic stratification required by the previously discussed relative sea-level and free air gravity data, and if the only forcing to which the system has been subject is that due to a glaciation-deglaciation cycle which ended ~ 7,000 BP.

Figure 3.17 illustrates the nature of the fit to the observed polar wander

Figure 3.17: Predictions of polar wander speed for six different parameterisations of the radial viscoelastic structure. The observed speed is shown as the cross

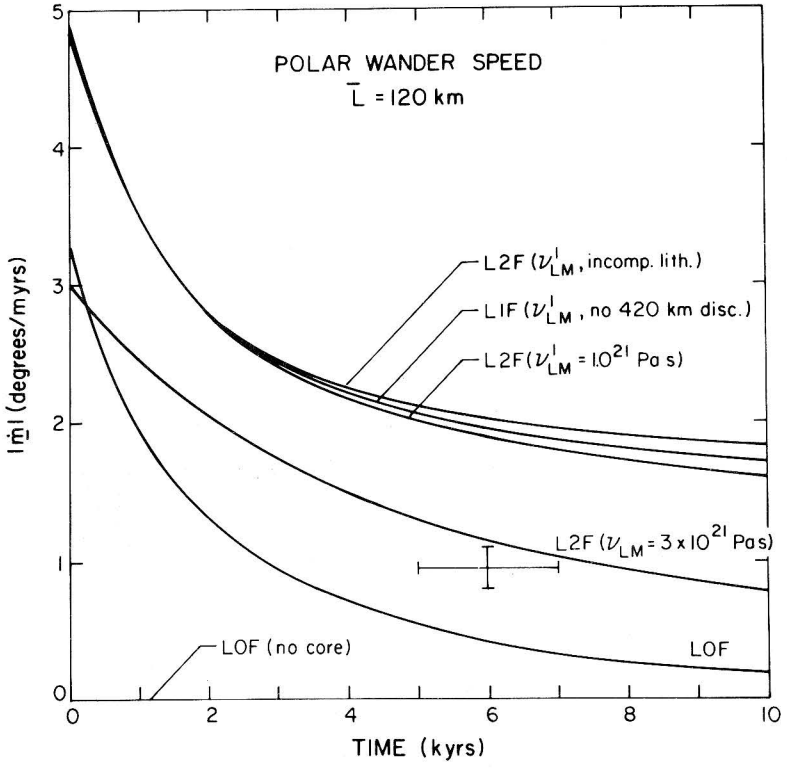

speed as a function of the viscoelastic model employed to make the prediction. Observations of oxygen isotope composition in deep-sea sedimentary cores (e.g. Fig. 3.8) are employed to constrain the cyclic variation of planetary ice cover which has occurred over the past 1 Ma. These data demonstrate that the major continental ice masses have appeared and disappeared in a highly periodic fashion, with a time interval of 100 ka separating successive interglacials (Fig. 3.8). Individual glaciation pulses in the sequence are each observed to have a saw-tooth form, with a slow glaciation period lasting ~ 90 ka followed by a fast collapse lasting 10 ka. The calculations illustrated in Figure 3.17 are based upon the assumption that seven such cycles have occurred and the observed polar wander speed of ~ 1° Ma^{-1} is shown at a time 6 ka following the last 10 ka disintegration event. Again this choice gives a best fit of the simple glaciation history model to the $\delta^{18}0$ data. Polar wander speed predictions are shown on this figure for six different viscoelastic models of the interior, each of which has the same lithospheric thickness $\bar{L}$ = 120 km. The prediction denoted by L0F (no core) is for the homogeneous model and verifies that the predicted speed following the end of the last deglaciation phase of the load cycle is essentially identical to zero, in accord with the theory of Munk and Revelle (1952). As radial structure is added to the model, however, the symmetry which enforces the null response in the homogeneous model is broken and the speeds predicted for times subsequent to the last glacial-deglacial pulse differ from zero. The effect of adding an inviscid high density core to the model is illustrated by the calculation denoted L0F, for which the elastic structure of the mantle is taken to be the average of model 1066B and the mantle viscosity is assumed to have the value 10^{21} Pa s. Model L1F includes in addition the influence of the density jump at 670 km depth in the earth, based upon the assumption that this discontinuity is capable of inducing a buoyant restoring force when it is displaced from equilibrium by the applied surface loads. The effect of this internal buoyancy in the mantle is further to increase the speed prediction in the model with 10^{21} Pa s uniform mantle viscosity. Adding a second density discontinuity at 420 km depth (model L2F with uniform viscosity) does not, however, produce a significant further increase in the speed prediction. The final calculation illustrated on Figure 3.17 (denoted L2F ($\nu_{LM} = 3 \times 10^{21}$ Pa s) demonstrates that the predicted speed can be reduced to the observed speed, simply by elevating the viscosity of the lower mantle to the same value required by the free air gravity and relative sea-level data discussed previously. As discussed in Wu and Peltier (1984) this model also correctly predicts the observed direction of polar wander. These results establish that the data shown in Figure 3.16 cannot be construed as requiring any currently ongoing variation in surface load, due to ice sheet disintegration on Greenland/Antarctica. Rather they are entirely explicable as a planetary memory of the last deglaciation event.

The final section of this chapter will focus, using the earth model whose properties have been fixed through analysis of the signatures of glacial isostasy discussed above, on the question of whether there is any evidence in modern tide gauge records of relative sea-level change for the operation of a current eustatic variation of sea level, due for example to ice sheet melting or thermal expansion.

SECULAR VARIATIONS OF RELATIVE SEA LEVEL WITH GLACIAL ISOSTASY REMOVED

It has been argued that the previously described global model of glacial isostasy is able to explain much of the observed variability in the record of relative sea-level change over the past 10 ka. Consequently it can be used to filter from the recent historical record of tide gauge observations of secular sea-level change that component which is due to this cause. One simply employs the data on the long timescale records of relative sea-level history (controlled by ^{14}C dating) to constrain the viscous component of mantle rheology. One then employs this earth structure to predict the present-day rate of sea-level rise/fall which should be observed at any location at which a tide gauge is installed, subtracts this prediction from the secular trend observed on the tide gauge and analyses the filtered data produced.

As a preliminary to this procedure it will be useful first to illustrate the continent scale variability of present-day relative sea-level variation predicted by the isostatic adjustment model. Figure 3.18 shows the present-day rate of sea-level rise/fall predicted for (a) North America and (b) Northwestern Europe, using an earth model with 1066B elastic structure. The viscous component of the model is one which has a lithospheric thickness of 200 km, an upper mantle viscosity of 10^{21} Pa s and a lower mantle viscosity of 2×10^{21} Pa s. This model provides a reasonably good fit to the ^{14}C record of relative sea-level rise along the US east coast when employed in conjunction with the ICE-2 deglaciation history of Wu and Peltier (1983) (Fig. 3 10). The meaning of the rates shown in the continental interior (where no ocean exists!) is that they represent the rates of separation between the surface of the solid earth and the geoid at such locations. Here the geoid is an imaginary surface continued inland from the oceans and on which the gravitational potential has the same value as obtains on the sea surface. Notable on these maps is the fact mentioned above, that the present-day maximum rates of relative sea-level fall in the regions which were once ice covered are near 1 cm a^{-1}. Surrounding each of the two main northern hemisphere centres of postglacial rebound, however, are ring-shaped regions in which relative sea-level is predicted to be rising at rates which may be as high as 2 mm a^{-1}; a maximum which obtains

Figure 3.18: Predicted present-day rates of relative sea-level rise (solid contours) and fall (dashed contours) for both (a) North America and (b) Europe, based upon an earth model with 1066B elastic structure, a lithospheric thickness of 200 km, an upper mantle viscosity of 10^{21} Pa s and a lower mantle viscosity of 2×10^{21} Pa s. For each map the contour interval Δ, in mm a^{-1}, is shown in the lower left-hand corner

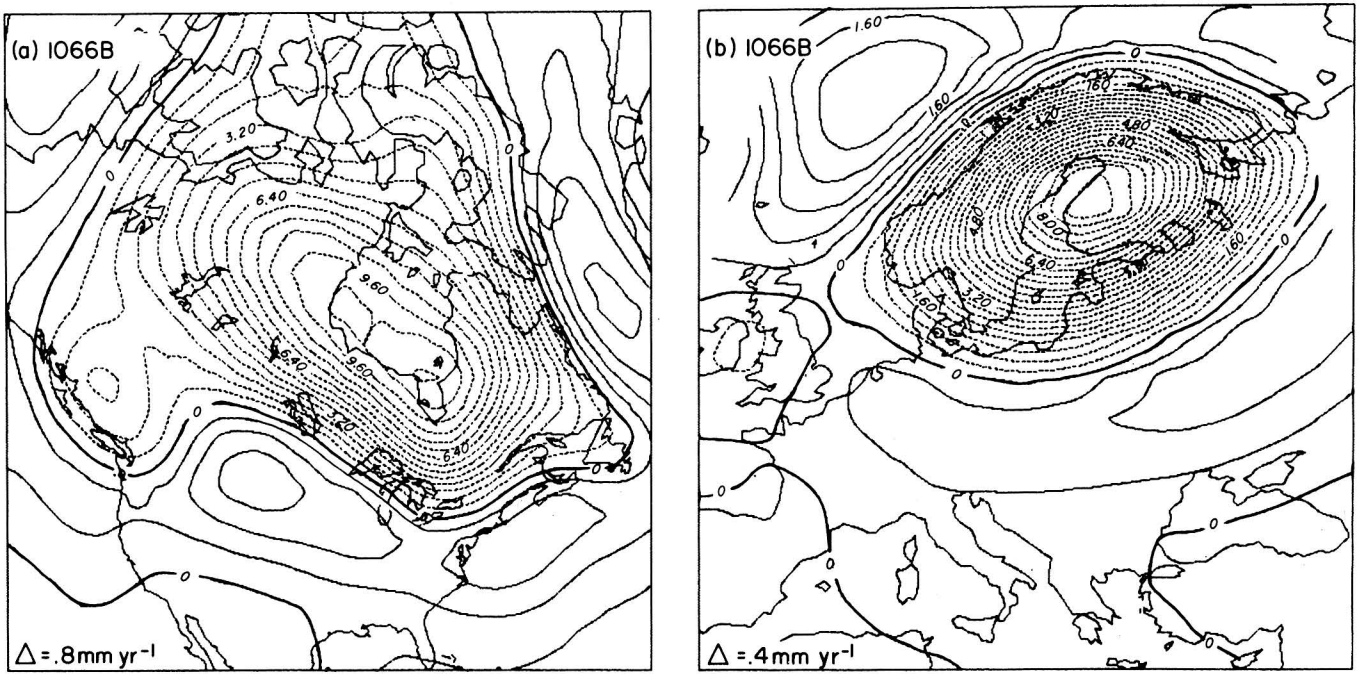

along the passive continental margin of the US east coast. The variation with position along the coast is fairly extreme, however, with very low values obtaining both to the north of the maximum and to the south. Notable also on this map is the fact that the predicted rates of glacial isostatic submergence along the US west coast are rather different from those on the east coast. The former region is much further distant from the main Laurentian ice mass and is also quite strongly influenced by the separate Cordilleran ice sheet, which existed west of the Canadian Rocky Mountains. As a consequence of these effects, the predicted variations of the rate of present-day relative sea-level change along this active continental margin are more complex.

Examination of Figure 3.18b illustrates a similar degree of complexity of the pattern of present-day RSL change predicted by the model for Northwestern Europe. The maximum present-day rates of relative sea-level fall near the centre of uplift in the Gulf of Bothnia is again near 1 cm a^{-1}. Surrounding this central region of uplift is the region of peripheral submergence. Again the latter region is very strongly asymmetric with respect to the former, just as in North America, a consequence of the geometric complexity of the distribution of water and land. One important feature of these results is the fact that rates of present-day sea-level rise are predicted to be much lower along the coast of France, which extends to the southwest away from the centre of uplift in Fennoscandia, than those along the east coast of the US which is similarly located with respect to the larger Laurentian ice mass.

Perhaps the most interesting aspect of these model predictions of the rates of present-day relative sea-level variation, induced by the last deglaciation event, is that they may be compared to direct tide gauge observations of these rates at any point of interest on the earth's surface. By way of illustration Figure 3.19 summarises the comparisons for all tide gauge sites on the east and west coasts of the continental US. The tide gauge observations employed in this figure consist of the secular trends extracted from the individual time series of observations at each gauge over the time interval 1940-80, as published in the recent catalogue of the National Ocean Service (1983). On Figure 3.19a, US east coast data, each cross represents the secular trend at a specific gauge corrected for the secular trend expected due to the influence of glacial isostatic adjustment. These corrected data are plotted as a function of the distance (in radians) of each gauge from the station at Key West, Florida, which is the southernmost station along the coast. The northernmost data point is for the gauge at Eastport, Maine. Also shown on this figure is the secular drift which has been subtracted from the raw data to make the correction for isostatic disequilibrium. This correction attains a maximum near 2 mm a^{-1} about midway along the coast, with very small rates obtaining at sites in Florida and Maine to the south and north of the maximum respectively. To give

Figure 3.19: Tide guage observed rates of relative sea-level rise, corrected for the influence of glacial isostatic adjustment, are shown as the dark crosses as a function of distance in radians measured from the southernmost tide gauge along the US east (a) and west (b) coasts. The three lines show the correction which was applied to remove the isostatic effect at each gauge. Note that the residual is biased to positive values along the east coast whilst there is no apparent bias on the west coast

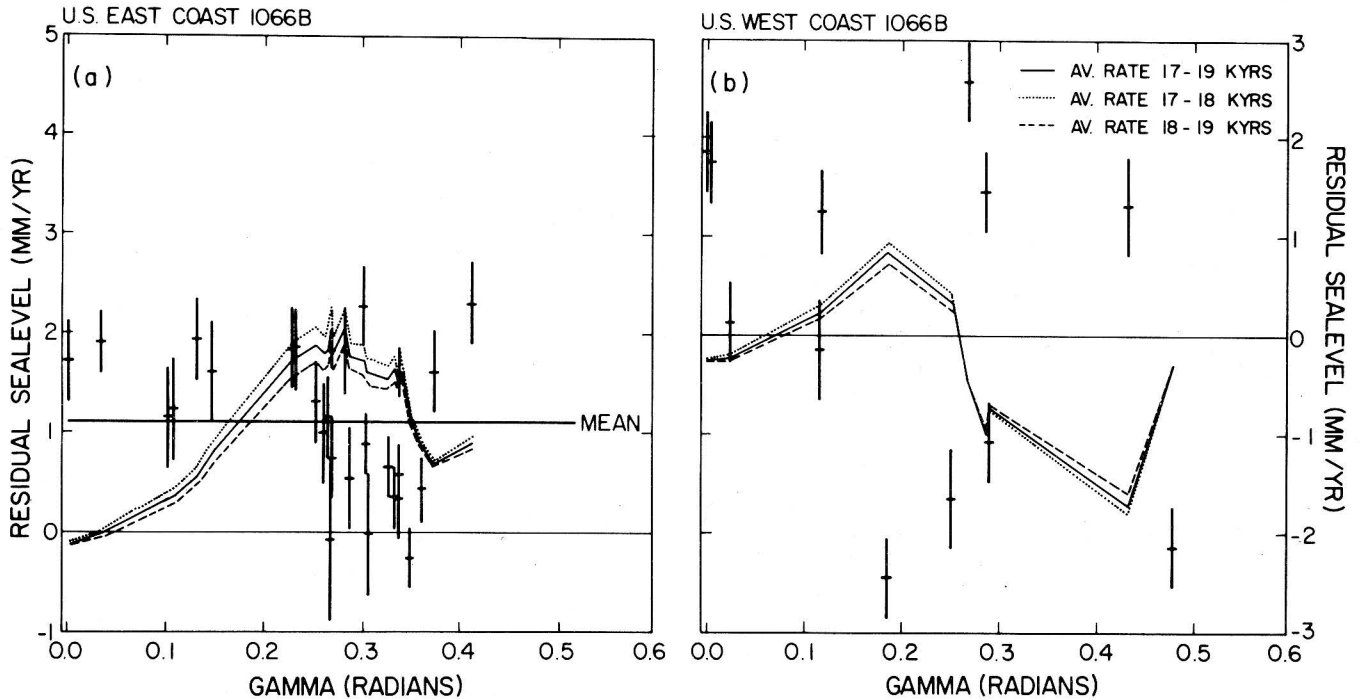

some indication of the error in the model predicted rates the predictions are shown not only for the present, 18 ka after glacial maximum, but also for 17.5 ka and 18.5 ka. Noticeable on these predicted curves are the several locations at which the predicted rates deviate from the smooth variation of rate with distance which otherwise obtains. These are sites at which errors due to the finite element discretisation occur (see Wu and Peltier, 1983, for a detailed discussion of the finite element discretisation employed to solve the sea-level equation).

The main point to note by inspection of the data (Fig. 3.19a) is that the correction, due to the influence of glacial isostasy, of the secular rate of relative sea-level rise along the US east coast accounts for as much as 100 per cent of the observed rate of rise at some sites. That is, at some sites along the US east coast, *all* of the observed secular rate of rise is explicable in terms of the influence of glacial isostatic adjustment. In general, however, there *is* a systematic misfit between the predicted rate of rise due to glacial isostasy and the rate of rise observed on an individual tide gauge, such that the observed rate of rise exceeds that predicted by the glacial isostatic adjustment model which fits the long timescale ^{14}C controlled relative sea-level histories. At no tide gauge along the US east coast is the observed rate of rise significantly slower than that predicted by the adjustment model. The average of the reduced rates of RSL rise at sites in this region is also shown on Figure 3.18a and is near 1.1 mm a^{-1}. The interpretation of this average in terms of a eustatic increase of sea level, either of steric or non-steric origin, is clearly made rather difficult by virtue of the fact that the residual trends vary erratically as a function of distance along the coast. Other physical processes must be contributing substantially to the secular variations of RSL which individual gauges are recording.

An identical treatment of the tide gauge data from the US west coast is shown on Figure 3.19b. Here the corrected tide gauge observed rates of RSL rise are shown as a function of position measured positive north from the southernmost gauge, which in this case is the one located at San Diego. The observations along this active continental margin are much more erratically scattered than those along the passive east coast continental margin, demonstrating the severe contamination of this record (for our present purposes) presumably as a result of local tectonic activity. Furthermore, the corrected data are scattered about zero and show no systematic bias toward positive rates as is evident for east coast sites. It would clearly be unreasonable to employ these data to make any inference whatsoever concerning eustatic sea-level variations.

CONCLUSIONS

In the previous sections of this chapter a number of the mechanisms responsible for producing changes in relative sea level have been discussed. The results of these changes have been classified as eustatic (deriving from the sea) or isostatic (deriving from the land). Although many changes in relative sea level are dominantly of either one type or the other, there do exist mechanisms which simultaneously induce both types of variation. The most important of these is that associated with the growth and decay of the vast continental ice sheets, whose appearance and disappearance has been a durable feature of the record of Pleistocene climatic change. Not only are there large eustatic variations of sea level associated with the transfer of mass from the oceans to the ice sheets and back again, but there are pronounced isostatic variations associated with the deformation of the earth induced by surface loading. These deformations in turn comprise both glacial isostatic (deriving from the ice) and hydro-isostatic (deriving from the water) contributions. Discussion in the chapter has tried to demonstrate the way in which a geophysical theory of the complex gravitational interactions, which ultimately determine postglacial relative sea-level change, can be exploited to infer important properties of the earth's interior on the basis of relative sea-level observations. These include not only aspects of the radial variation of viscosity, such as the thickness of the surface lithosphere and the value of the sub-lithospheric viscosity, but also the extent to which the density variation with depth in the mantle is adiabatic or non-adiabatic. Further, an attempt has been made to show how this model can be employed to filter deglaciation induced relative sea-level variations from modern tide gauge records of secular sea-level change, and so enable us to see more clearly any other climatological signal which may be present in these records. A great deal is left to be done before we will be in any position to claim a complete understanding of the full spectrum of sea-level variability. However, the record has already yielded an impressive collection of insights into the way in which the earth works.

REFERENCES

Barnett, T.P. (1983a) 'Possible changes in global sea level and their causes', *Climate Change, 5(1)*, 15-38.

—— (1983b) 'Long term changes in dynamic heights', *J. Geophys. Res., 88*, 9547-52.

Bloom, A.L. (1967) 'Pleistocene shorelines: A new test of isostasy', *Bull. Geol. Soc. Am., 78*, 1477-93.

—— (1970) 'Paludal stratigraphy of Truk, Ponape, and Kusaie, Eastern Caroline Islands', *Bull. Geol. Soc. Am., 81*, 1895-904.

—— (1983) 'Sea-level and coastal morphology through the Late Wisconsin glacial maximum', in S.C. Porter (ed.), *Late Quaternary Environments of the United States, Vol. 1 — The Late Pleistocene*, Longman, London, pp. 215-29.

Carter, W.E. and Robertson, D.S. (1986) 'Earth rotation from VLBI measurements', in A.J. Anderson and A. Cazanave (eds), *Space Geodesy and Geodynamics*, Academic Press, London and New York, pp. 85-96.

—— Robertson, D.S., Pyle, T.E. and Diamante, J. (1986) 'The application of geodetic radio interferometric surveying to the monitoring of sea level', *Geophys. J. Roy. Astron. Soc., 87*, 3-13.

Clark, J.A., Farrell, W.E. and Peltier, W.R. (1978) 'Global changes in postglacial sea level: A numerical calculation', *Quat. Res., 9*, 265-87

Cox, A. and Dalrymple, G.B. (1967) 'Statistical analysis of geomagnetic reversal data and the precision of potassium-argon dating', *J. Geophys. Res., 72*, 2603-14.

Csanady, G.T. (1982) *Circulation in the Coastal Ocean*, Reidel, Dordrecht.

Dziewonski, A.M. and Anderson D.L. (1981) 'Preliminary reference earth model', *Phys. Earth Planet. Int., 25*, 297-356.

Fairbridge, R.W. (1976) 'Shellfish-eating pre-ceramic Indians in coastal Brazil', *Science, 191*, 353-9.

Farrell, W.E. and Clark, J.A. (1976) 'On postglacial sea level', *Geophys. J. Roy. Astron. Soc., 46*, 647-67.

Geodynamics Program Office (1983), *The NASA Geodynamics Program, an Overview*, NASA Technical Paper No. 2147.

—— (1984), *NASA Geodynamics Program: Fifth Annual Report*, NASA Technical Memorandum, 87359

Gilbert, F. and Dziewonski, A.M. (1975) 'An application of normal mode theory to the retrieval of structural parameters and source mechanisms from seismic spectra', *Phil. Trans. Roy. Soc. Lond., A, 276*, 187-269.

Gill, E.D. (1965) 'Radiocarbon dating of past sea levels in SE Australia', *Abstracts, INQUA VII Congress*, Boulder, Col., p. 167.

Gornitz, V., Lebedeff, L. and Hansen, J. (1982) 'Global sea level trend in the past century', *Science, 215*, 1611-14.

Hansen, J., Johnson, D., Lacis, A., Lebedeff, S., Lee, P., Reid, D. and Russell, G. (1981) 'Climate impact of increasing atmospheric carbon dioxide', *Science, 213*, 957-66.

Hays, J.D., Imbrie, J. and Shackleton, N.J. (1976) 'Variations in the earth's orbit: Pacemaker of the ice ages', *Science, 194*, 1121-32.

Hyde, W.T. and Peltier, W.R. (1985). 'Sensitivity experiments with a model of the ice age cycle: the response to harmonic forcing', *J. Atmos. Sci.*, (September).

Imbrie, J., Van Donk, J. and Kipp, N.G. (1973) 'Paleoclimatic investigation of a Late Pleistocene Caribbean deep-sea core: Comparison of isotopic and faunal methods', *Quat. Res. (NY, 3*, 10-38.

Imbrie, J., Shackleton, N.J., Pisias, N.G., Morley, J.J., Prell, W.L., Martinson, D.G., Hays, J.D., McIntyre, A. and Mix, A.C. (1984) 'The orbital theory of Pleistocene climate: Support from a revised chronology of the marine $\delta^{18}0$ record', in A. Berger, J. Imbrie, J. Hays, G. Kukla and B. Saltzman (eds), *Milankovitch and Climate*, Reidel, Dordrecht, vol. I. pp. 269-305.

Jelgersma, S. (1966) 'Sea level changes during the last 10,000 years', in *Proceedings of the International Symposium on World Climate from 8000 to 0 BX*, Royal Meteorological Society, London, pp. 54-71.

Lagios, E. and Wyss, M. (1983) 'Estimates of vertical crustal movements along the coast of Greece, based upon mean sea level data', *PAGEOPH, 121*, 869-87.

Lowe, J.J. and Walker, M.J.C. (1984) *Reconstructing Quaternary Environments*, Longman, London.

Mareschall, J.-C and Gangi, A.F. (1977) 'Equilibrium position of phase boundary under horizontally varying surface loads', *Geophys. J. Roy. Astron. Soc., 49*, 757-72.

Marsh, J.G. and Martin, T.V. (1982) 'The SEASAT altimeter mean sea surface model', *J. Geophys. Res., 87*, 3269-80.

Meier, Mark F. (1984) 'Contribution of small glaciers to global sea level', *Science, 226*, 1418-21.

Milankovitch, M. (1941) *Canon of Insolation and the Ice-Age Problem*, K. Serb. Akad. Geogr., Spec. Publ. No. 132, translated by Israel Program for Scientific Translations, Jerusalem, 1976, US Department of Commerce.

Munk, W.H. and Revelle, R. (1952) 'On the geophysical interpretation of irregularities in the rotation of the Earth', *Mon. Not. Roy. Astron. Soc., Geophys. Suppl., 6*, 331-47.

National Ocean Service (1983) *Sea Level Variations for the United States 1855-1980*, US Department of Commerce, National Oceanic and Atmospheric Administration, Rockville, Md.

Noble, M. and Butman, B. (1979) 'Low frequency wind induced sea level oscillations along the east coast of North America', *J. Geophys. Res., 84*, 3227-36.

O'Connell, R.J. (1976) 'The effects of mantle phase changes on postglacial rebound', *J. Geophys. Res., 81*, 971-4.

Peltier, W.R. (1974) 'The impulse response of a Maxwell Earth', *Rev. Geophys. Space Phys., 12*, 649-69

—— (1976) 'Glacio-Isostatic adjustment–II. The inverse problem', *Geophys. J. Roy. Astron. Soc., 46*, 669-706.

—— (1980) 'Mantle convection and viscosity', in A.M. Dziewonski and E. Boschi (eds), *Physics of the Earth's Interior*, North Holland, Amsterdam, pp. 362-431.

—— (1981) 'Ice age geodynamics', *Ann. Rev. Earth Planet. Sci., 9*, 199-225.

—— (1982) 'Dynamics of the Ice Age Earth', *Adv. Geophys., 24*, 1-146.

—— (1983) 'Constraint on deep mantle viscosity from LAGEOS acceleration data', *Nature, 304*, 434-6.

—— (1984a) 'The rheology of the planetary interior', *Rheology, 28*, 665-97.

—— (1984b) 'The thickness of the continental lithosphere', *J. Geophys. Res., 89*, 11,303-16.

—— (1985a) 'The LAGEOS constraint on deep mantle viscosity: results from a new normal mode method for the inversion of viscoelastic relaxation spectra', *J. Geophys. Res., 90*, B11, 9411-21.

—— (1985b). 'Mantle convection and viscoelasticity', *Ann. Rev. Fluid. Mech., 17*, 561-608.

—— and Andrews, J.T. (1976) 'Glacial isostatic adjustment I: The forward problem', *Geophys. J. Roy. Astron. Soc., 46*, 605-46.

—— Farrell, W.E. and Clark, J.A. (1978) 'Glacial isostasy and relative sea level: a global finite element model', *Tectonophys., 50*, 81-110.

—— Wu, Patrick and Yuen, D.A. (1981) 'The Viscosities of the planetary mantle', in F.D. Stacey, A. Nicholas and M.S. Paterson (eds), *Anelasticity in the Earth*, American Geophysical Union, Washington, DC.

—— and Wu, Patrick (1982) 'Mantle phase transitions and the free air gravity anomalies over Fennoscandia and Laurentia', *Geophys. Res. Lett., 9*, 731-734.

—— and Wu, Patrick (1983). Continental lithospheric thickness and deglaciation induced true polar wander. *Geophys. Res. Lett., 10*, 181-4.

—— and Hyde, W.T. (1984) 'A model of the ice age cycle', in A. Berger, J.

Imbrie, J. Hays, G. Kukla and B. Saltzman (eds), *Milankovitch and Climate*, Reidel, Dordrecht, vol. II, pp. 565-80.

Rapp, R.H. (1979) 'Geos 3 data processing for the recovery of geoid undulations and gravity anomalies' *J. Geophys. Res., 84*, 3784-92.

Roemmich, D. and Wunsch, C. (1984) 'Apparent changes in the climatic state of the deep North Atlantic Ocean', *Nature, 307*, 447-50.

Russell, R.J. (ed.) (1961) 'Pacific Island Terraces: Eustatic?' *Zeit. Geomorph. Suppl., 3.*

Sabadini, R. and Peltier, W.R. (1981) 'Pleistocene deglaciation and the earth's rotation: implications for mantle viscosity', *Geophys. J. Roy. Astron. Soc., 66*, 552-78.

Schofield, J.C. (1964) 'Post-glacial sea levels and isostatic uplift', *NZ J. Geol. Geophys., 7*, 359-70.

Schutz, E.B., Tapley, B.D. and Shum, C. (1982) 'Evaluation of the SEASAT altimeter time tag bias', *J. Geophys. Res., 87*, 3239-45.

Shackleton, N.J. and Opdyke, N.D. (1973) 'Oxygen isotope and paleomagnetic stratigraphy of equatorial Pacific core V28-238: Oxygen isotope temperatures and ice volumes on a 10 to 10^6 year timescale', *Quat. Res., 3*, 39-54.

—— and Opdyke, N.D. (1976) 'Oxygen isotope and paleomagnetic stratigraphy of Pacific core V28-239 late Pleistocene to latest Pleistocene', *Mem. Geol. Soc. Am., 145*, 449-64.

Shepard, F.P. (1963) 'Thirty-five thousand years of sea level', in T. Clements (ed.), *Essays in Marine Geology*, University of Southern California Press, Los Angeles, Calif., pp. 1-10.

Stanley, H.R. (1979) 'The Geos 3 project', *J. Geophys. Res., 84*, 3779-83.

Thompson, K.R. (1981) 'Monthly changes of sea level and the circulation of the North Atlantic', *Ocean Modelling, 41*, 6-9.

Vincent, R.O. and Yumi, S. (1969, 1970) 'Co-ordinates of the pole (1899-1968), returned to the conventional international origin', *Publ. Int. Latitude Observ. Mizusawa, 7*, 41-50.

Weertman, J. (1978) 'Creep laws for the mantle of the Earth', *Phil. Trans. Roy. Soc. Lond., A288*, 9-26.

Wu, Patrick, and Peltier, W.R. (1983) 'Glacial isostatic adjustment and the free air gravity anomaly as a constraint on deep mantle viscosity', *Geophys. J. Roy. Astron. Soc., 74*, 377-449.

—— and W.R. Peltier (1984) 'Pleistocene deglaciation and the Earth's rotation: a new analysis', *Geophys. J. Roy. Astron. Soc., 76*, 753-92.

Wunsch, C. (1981) 'An interim relative sea surface for the North Atlantic ocean', *Mar. Geodesy, 5*, 103-19.

—— and Gaposhkin, E.M. (1980) 'On using satellite altimetry to determine the general circulation of the oceans with applications to geoid improvement', *Rev. Geophys. Space Phys., 18*, 725-45.

Wyrtki, K. and Nakahara, S. (1984) *Monthly Maps of Sea Level Anomalies in the Pacific 1975-1981*, Hawaii Institute of Geophysics Report HIG-84-3.

Wyss, M. (1976a). 'Local sea level changes before and after the Hyuganada, Japan earthquakes of 1961 and 1968', *J. Geophys. Res., 81*, 5315-21.

—— (1976b) 'Local changes of sea level before large earthquakes in South America', *Bull. Seis. Soc. Am., 66*, 903-14.